ARL-TR-7513 ● OCT 2015

US Army Research Laboratory

Harmonic Phase Response of Nonlinear Radar Targets

by Sean F McGowan, Dr Gregory J Mazzaro,
Kelly D Sherbondy, and Ram M Narayanan

NOTICES

Disclaimers

The findings in this report are not to be construed as an official Department of the Army position unless so designated by other authorized documents.

Citation of manufacturer's or trade names does not constitute an official endorsement or approval of the use thereof.

Destroy this report when it is no longer needed. Do not return it to the originator.

ARL-TR-7513 ● OCT 2015

US Army Research Laboratory

Harmonic Phase Response of Nonlinear Radar Targets

by Sean F McGowan and Kelly D Sherbondy
Sensors and Electron Devices Directorate, ARL

Dr Gregory J Mazzaro
Department of Electrical & Computer, Engineering, The Citadel, The Military College of South Carolina, 171 Moultrie St, Charleston, SC 29409

Ram M Narayanan
Professor of Electrical Engineering, 202 Electrical Engineering East Building, The Pennsylvania State University, University Park, PA 16802, USA

REPORT DOCUMENTATION PAGE

Form Approved
OMB No. 0704-0188

1. REPORT DATE *(DD-MM-YYYY)*	2. REPORT TYPE	3. DATES COVERED (From - To)
October 2015	Final	08/2015

4. TITLE AND SUBTITLE
Harmonic Phase Response of Nonlinear Radar Targets

5a. CONTRACT NUMBER

5b. GRANT NUMBER

5c. PROGRAM ELEMENT NUMBER

6. AUTHOR(S)
Sean F McGowan, Dr Gregory J Mazzaro, Kelly D Sherbondy, and Ram M Narayanan

5d. PROJECT NUMBER

5e. TASK NUMBER

5f. WORK UNIT NUMBER

7. PERFORMING ORGANIZATION NAME(S) AND ADDRESS(ES)
US Army Research Laboratory
ATTN: RDRL-SER-U
2800 Powder Mill Road
Adelphi, MD 20783-1138

8. PERFORMING ORGANIZATION REPORT NUMBER
ARL-TR-7513

9. SPONSORING/MONITORING AGENCY NAME(S) AND ADDRESS(ES)

10. SPONSOR/MONITOR'S ACRONYM(S)

11. SPONSOR/MONITOR'S REPORT NUMBER(S)

12. DISTRIBUTION/AVAILABILITY STATEMENT
Approved for public release; distribution is unlimited.

13. SUPPLEMENTARY NOTES

14. ABSTRACT
One of the latest challenges being investigated by the US Army Research Laboratory's (ARL) Electronics and Radio Frequency (E&RF) Division is the development of a radar system that can accurately detect and range an electronically nonlinear target, such as a detonator of an improvised explosive device (IED). Previous nonlinear radar systems detect targets via transmission of a single frequency ω, stepping (incrementally increasing) this frequency through a wide bandwidth, and then listening for a response of the 2nd harmonic 2ω; however, the phase information that this harmonic contains and its relationship to target distance has been largely assumed and unconfirmed. Our most recent experimental tests, both wired and wireless, have confirmed that this harmonic phase response is constant versus frequency at the target. Using inverse Fourier transforms, the range of an electronic nonlinear target can be determined from that phase.

15. SUBJECT TERMS
nonlinear, phase, ranging

16. SECURITY CLASSIFICATION OF:			17. LIMITATION OF ABSTRACT	18. NUMBER OF PAGES	19a. NAME OF RESPONSIBLE PERSON
a. REPORT	b. ABSTRACT	c. THIS PAGE			Kelly D Sherbondy
Unclassified	Unclassified	Unclassified	UU	36	19b. TELEPHONE NUMBER (Include area code) 301-394-2533

Contents

List of Figures

List of Tables

Acknowledgments

I appreciate the mentorship of Dr Anthony Martone and Mr Kelly Sherbondy. I would also like to thank Dr Andy Sullivan, Dr Matthew Higgins, Dr Gregory Mazzaro, Mr Marc Ressler, Mr Edward Viveiros, Dr Ronald Polcawich, Mr Brian Phelan, Mr Kyle Gallagher, and Mr Roger Cutitta for their assistance and support. I also wish to acknowledge my fellow interns Richard Pooler, Kristopher Young, Jason Cornelius, and Philip Saponaro.

Student Bio

Sean F McGowan is a senior undergraduate at Pennsylvania State University pursuing a BS degree in electrical engineering through Penn State's Schreyer Honors College. It is his first summer interning at the US Army Research Laboratory, though he has worked in Penn State's Optics & Laser Lab earlier in his undergraduate career. In the future he hopes to further his education by attending graduate school and obtaining his Masters in electrical engineering, with a focus on signal processing.

INTENTIONALLY LEFT BLANK.

1. Introduction/Background

Unlike its traditional, linear counterpart, nonlinear radar offers the ability to detect and range targets that contain electronically nonlinear components, such as transistors, diodes, and semiconductors. While many circuit devices, such as amplifiers, mixers, and converters, exhibit nonlinear behavior, the true potential of nonlinear radar is shown in its real-world application of detecting a range of targets from handheld radios to electronic detonators of improvised explosive devices (IEDs). Targets such as these are difficult to detect with linear radar, due to their typical size and shape – often small and thin, with a slim geometric profile. This profile lends itself to a small radar cross section, which can easily be obscured and interfered with by nearby objects or clutter. Nonlinear radar offers the feature of high clutter rejection, but this must be weighed against 2 disadvantages: 1) the harmonic response from the target is extremely weak, and thus difficult to capture, and 2) the incident power required to generate a detectable response is significantly higher than that of linear radar.[1,2]

The nonlinear radar model used in my experiments is akin to a harmonic, stepped frequency radar. The radar transmits a single frequency, ω; if the radar receives a harmonic of this fundamental (i.e., 2ω and 3ω), a nonlinear target is present. The original fundamental frequency ω is then stepped, or increased by an increment $\Delta\omega$, across a bandwidth until enough harmonic data are collected to verify detection and calculate distance to target.[3]

A general diagram of harmonic radar is shown in Fig. 1. In the transmission chain, the fundamental ω is amplified to increase its incident power on the target, and then fed through a low pass filter to attenuate any artifacts created from amplification. This signal is then transmitted to a target, and then reflected back to the receive chain, the effective reverse of the transmission chain. This time, the signal is fed through a high pass filter to attenuate the fundamental, while allowing its harmonics to pass through. The weak harmonic responses are then amplified to allow for easier detection and measurement.

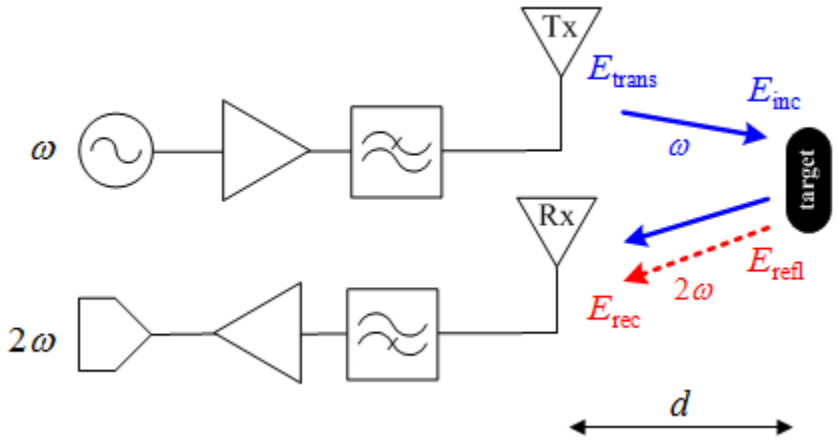

Fig. 1 General model of harmonic radar,[3] where transmitter = Tx and receiver = Rx

In earlier studies of nonlinear radar, the phase of these reflected harmonics has largely been assumed to be constant versus the bandwidth of frequencies transmitted to the target.[3] This previously unconfirmed relationship is necessary to calculate the distance to target using an inverse Fourier transform. My experimental designs reexamine this assumption to affirm it and uphold that the harmonic stepped-frequency methods of radar are widely applicable for the detection and ranging nonlinear targets.

2. Harmonic Phase Response Theory

Let the transmitted electric field be a single-frequency sinusoid, represented as a complex exponential:

$$E_{\text{trans}}(t) = E_{\text{t}} e^{j\phi_{\text{t}}} e^{j\omega t} \tag{1}$$

Equation 1 shows E_{t} and ϕ_{t} as the initial amplitude and phase of the transmitted electric field, and ω is its fundamental frequency in radians.

As the transmitted wave travels a distance d to the target in time τ, the amplitude of its electric field will attenuate as it propagates through the lossy medium, such as a transmission line or air. Additional, the wave will undergo a phase shift that proportional to its operating frequency. Arriving at the target, the incident electric field may be written as

$$E_{\text{inc}}(t) = E_{\text{i}} e^{-j\omega\tau} e^{j\omega t} \tag{2}$$

where $E_i < E_t$. The incident electric field incident E_{inc} can be related to the electric field that reflects off the target by the standard power series model for nonlinear, memoryless targets:[12–15]

$$E_{\text{refl}}(t) = \sum_{p=1}^{\infty} \tilde{a}_p E_{\text{in}}^p(t) \tag{3}$$

where a_p are complex power-series coefficients. The value of a_1 is the linear response of the target, whereas the following coefficients $\{a_2, a_3, \ldots\}$ depend on a variety of properties of the device, such as the specific clutter around the device, the orientation of the target, and other radio frequency (RF) interference in the environment.

When the incident electric field described in Eq. 2 is substituted into Eq. 3, and the expanded, the result is

$$\begin{aligned} E_{\text{refl}}(t) &= \tilde{a}_1 E_{\text{i}}\, e^{-j\omega\tau} e^{j\omega t} + \tilde{a}_2 E_{\text{i}}^2 e^{-j2\omega\tau} e^{j2\omega t} + \tilde{a}_3 E_{\text{i}}^3 e^{-j3\omega\tau} e^{j3\omega t} + \ldots \\ &= \left|a_1\right| e^{j\phi_1} E_{\text{i}}\, e^{-j\omega\tau} e^{j\omega t} + \left|a_2\right| e^{j\phi_2} E_{\text{i}}^2 e^{-j2\omega\tau} e^{j2\omega t} + \left|a_3\right| e^{j\phi_3} E_{\text{i}}^3 e^{-j3\omega\tau} e^{j3\omega t} + \ldots \end{aligned} \tag{4}$$

This is the reflected electric field, the wave after the transmitted signal has reached the target and begins to travel back to the radar's receiver. Assuming the radar is monostatic (the transmitter and receiver are combined and thus the same distance to the target), the reflected electric field will experience a second, identical time delay of τ on its return, so that the electric field received can be described as

$$\begin{aligned} E_{\text{rec}}(t) &= \left[E_1 e^{j\phi_1} e^{-j\omega\tau} e^{j\omega t}\right] e^{-j\omega\tau} + \left[E_2 e^{j\phi_2} e^{-j2\omega\tau} e^{j2\omega t}\right] e^{-j2\omega\tau} + \ldots \\ &= \left(E_1 e^{j\omega t}\right)\left(e^{-j2\omega\tau} e^{j\phi_1}\right) + \left(E_2 e^{j2\omega t}\right)\left(e^{-j4\omega\tau} e^{j\phi_2}\right) + \left(E_3 e^{j3\omega t}\right)\left(e^{-j6\omega\tau} e^{j\phi_3}\right) + \ldots \\ &= \sum_{M=1}^{\infty} E_M e^{jM\omega t} \cdot e^{-j\left(2M\omega\tau - \phi_M\right)} \end{aligned} \tag{5}$$

In Eq. 5, E_M denotes the electric-field amplitude received at each harmonic M of fundamental frequency ω. Each harmonic of the stepped fundamental frequency experiences a phase delay of $2M\omega\tau - \phi_M$. This delay is the key phase information needed to obtain range-to-target data.

If we describe Eq. 5, the electric field received by the radar, as a phasor, the result is the complex equation

$$\tilde{E}_{\text{rec}}(M\omega) = E_M \angle\left\{\phi_M - 2M\omega\tau\right\}. \tag{6}$$

To obtain distance from the equation, a simple substitution of $\tau = d/u_p$ is required. This relationship simply states the time it take for wave to travel to the target is the distance to the target divided by the wave's speed.

$$\tilde{E}_{\text{rec}}(M\omega) = E_M \angle\left\{\phi_M - 2M\omega\left(d/u_p\right)\right\} . \tag{7}$$

Finally, range-to-target may be calculated by solving for the derivative of the phase of E_{rec} with respect to radian frequency of the fundamental. However, this is only true of the harmonic phase response from the target is constant versus frequency.

$$\begin{aligned} \angle\tilde{E}_{\text{rec}}(M\omega) &= \phi_M - 2M\omega\left(d/u_p\right) \\ \frac{\partial}{\partial\omega}\angle\tilde{E}_{\text{rec}} &= 0 - 2M\frac{d}{u_p} \\ d &= -\frac{u_p}{2M}\left\{\frac{\partial}{\partial\omega}\angle\tilde{E}_{\text{rec}}\right\} . \end{aligned} \tag{8}$$

The experimental data collected and delineated in this study confirm that target distance can be calculated from E_{rec} using Eq. 8.

3. Wireline Experiment

To begin verification of the assumed phase-frequency relationship, a basic wireline experimental design is used, as depicted in Fig. 2. Both the radar's transmitter and receiver is simulated by using the Keysight N5242A PNA-X nonlinear vector network analyzer (NVNA). The NVNA transmits a series of stepped signals from Port 1 along 2 cascaded 12-ft MegaPhase F130 transmission lines, whose loss and distortion is known. These cables simulate the distance between the radar and a nonlinear target. The incident signal, notated as A1, reaches the target, and is reflected back into Port 1 of the NVNA, as B1.

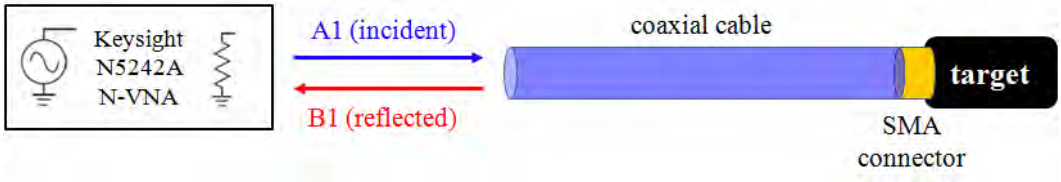

Fig. 2 Wireline experimental setup[3]

The targets used in this wireline experiment are as follows:

- MiniCircuits ZX60-3011+ amplifier (input port)
- MiniCircuits ZX60-V63+ amplifier (input port)
- MiniCircuits ZLW-186MH mixer (RF port)
- MiniCircuits ZFM-2000+ mixer (RF port)
- Motorola FV300 radio (antenna port)

- Motorola T4500 radio (antenna port)

Each target had SMA input and output ports. For the amplifiers and mixers, unused ports were terminated with a 50-Ω load. For the Motorola handheld radios, their antennas were replaced with an SMA end launch soldered to their printed circuit board (PCB). Every target exhibits nonlinear behavior, with the amps and mixers typically being components to detect in a larger electronic target, and the radios more accurately representing a real-world target for a nonlinear radar system to detect.

For this wireline experiment, the previously derived distance, Eq. 8, can be simplified to account for the wave's propagation through a lossy cable like the MegaPhase F130s.

$$d = -\frac{u_p}{2M}\left\{\frac{\partial}{\partial\omega}\angle \mathrm{B1}\right\} = -\frac{c/\sqrt{\varepsilon_r}}{2M}\left\{\frac{\phi_M(\omega_2)-\phi_M(\omega_1)}{\omega_2-\omega_1}\right\} \tag{9}$$

In Eq. 9, the propagation speed has been broken down to the speed of light and the dielectric constant of the transmission line. Additionally, the derivative of the phase of the return wave has been simplified to a discrete slope equation between 2 collected data points.

Finally, the sweep the NVNA transmits to the target is from 800 to 900 MHz with a 1.25-MHz step. Each transmitted sinusoid has the same amplitude, but is applied to the target at 2 different power levels: –10 and 0 dBm. The results are displayed Figs. 3 through 15, with the frequency reported in Hz.

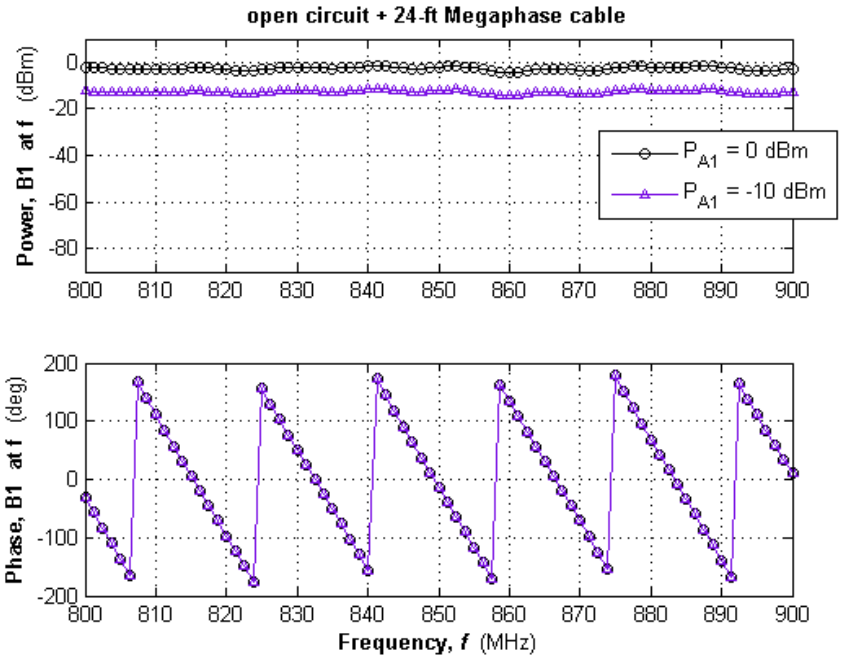

(a)

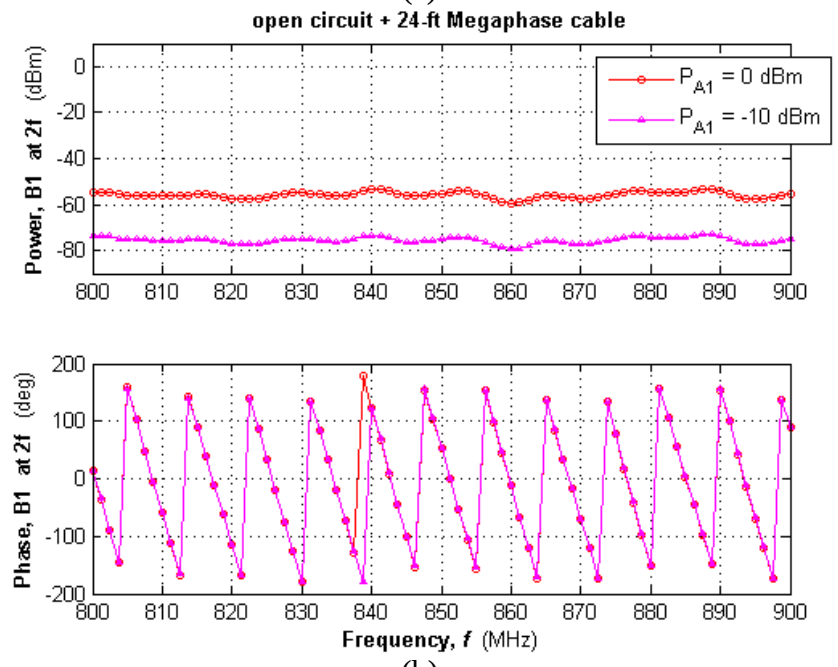

(b)

Fig. 3 Power and phase of reflection from the 24-ft cable with open-circuit termination at a) fundamental and b) 2nd harmonic[3]

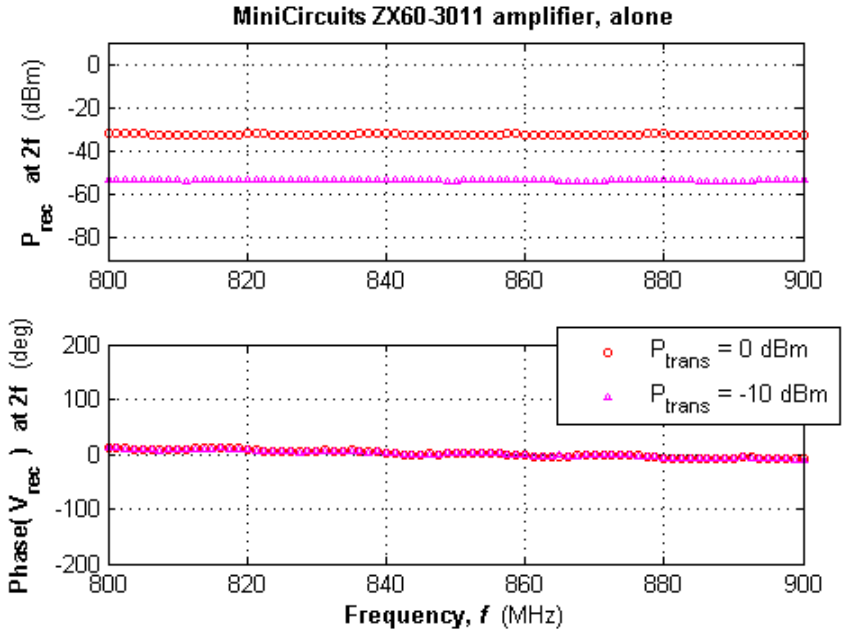

(a)

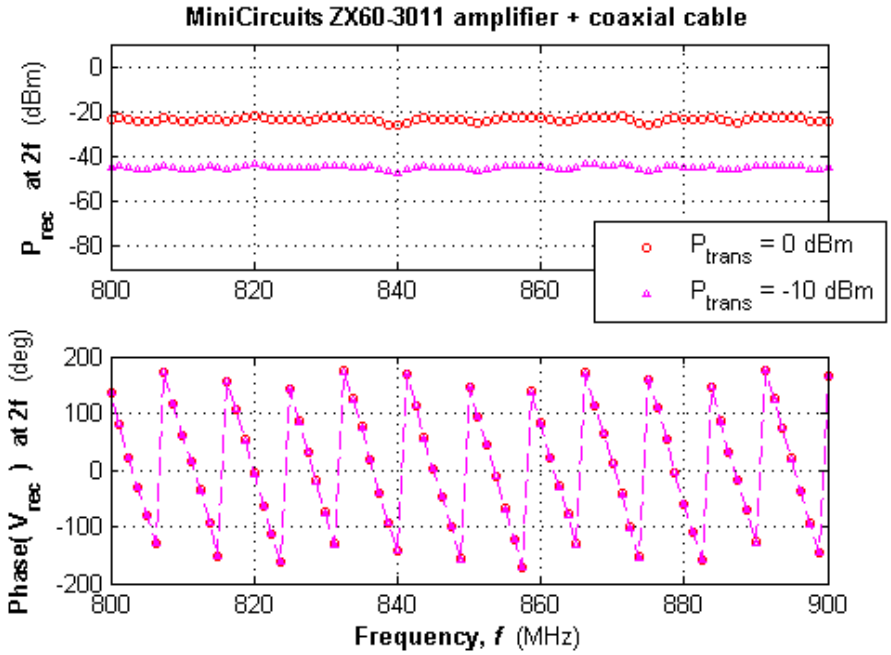

(b)

Fig. 4 Power and phase of 2nd harmonic reflection from ZX60-3011 amp input: a) amp connected to Port 1 and b) amp connected through the 24-ft cable to Port 1

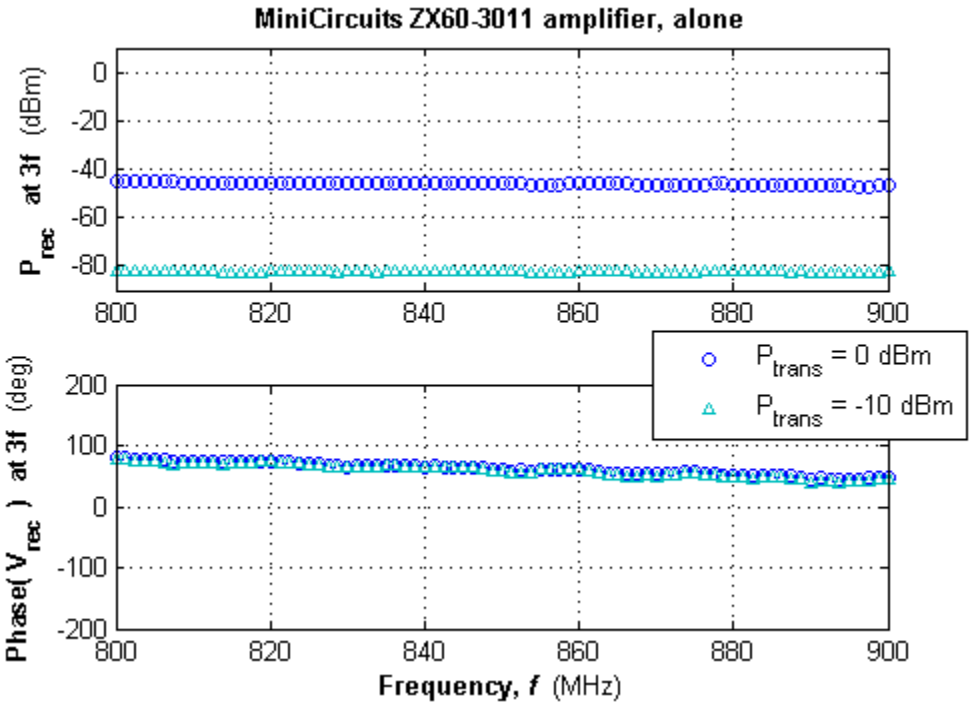

(a)

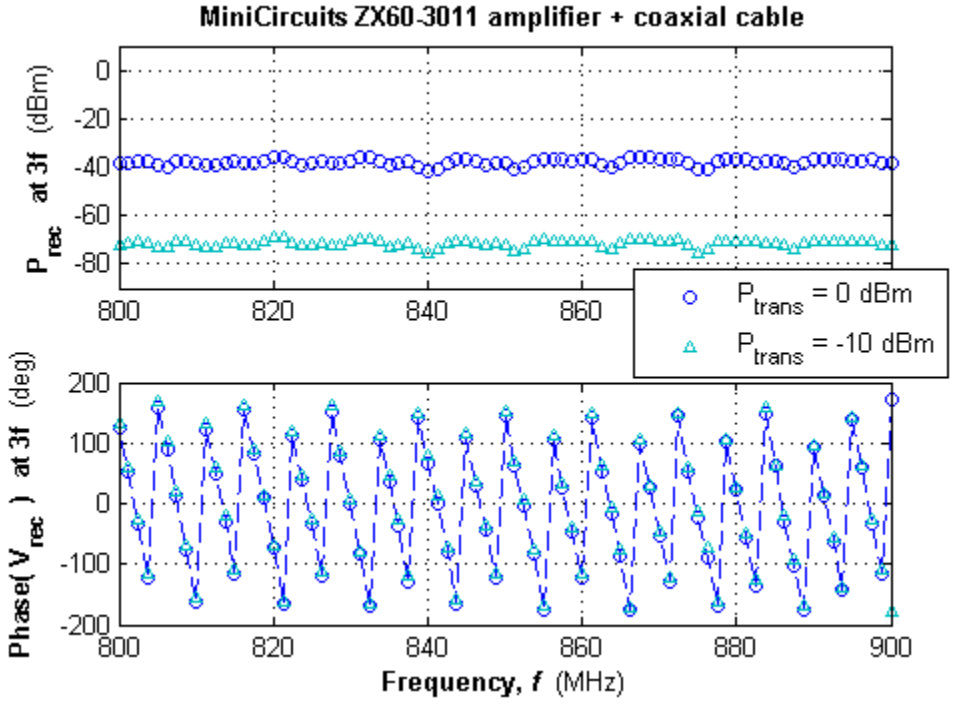

(b)

Fig. 5 Power and phase of 3rd harmonic reflection from the ZX60-3011 amp input: a) amp connected to Port 1 and b) amp connected through the 24-ft cable to Port 1

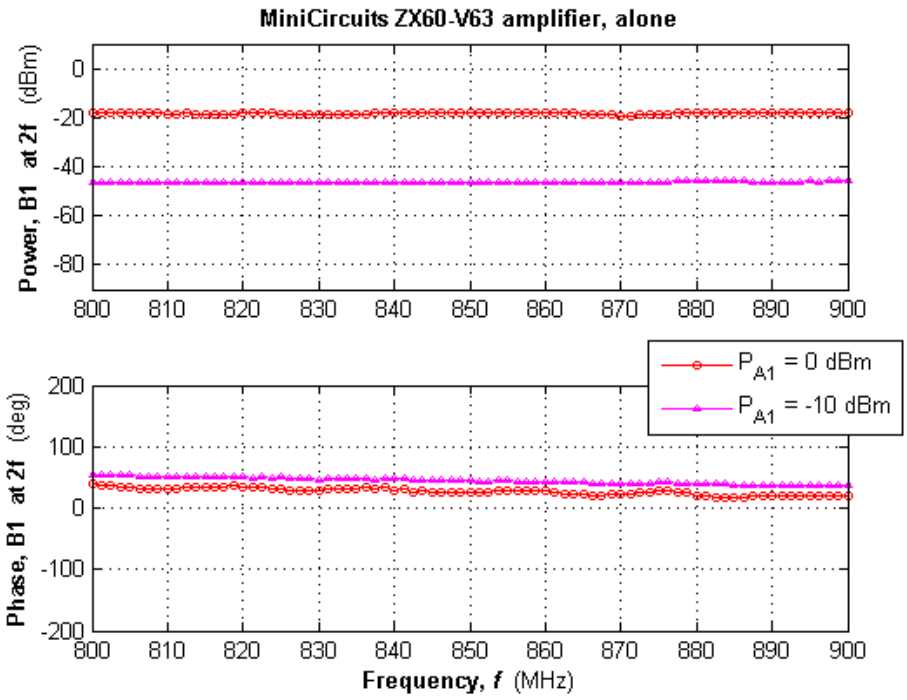

(a)

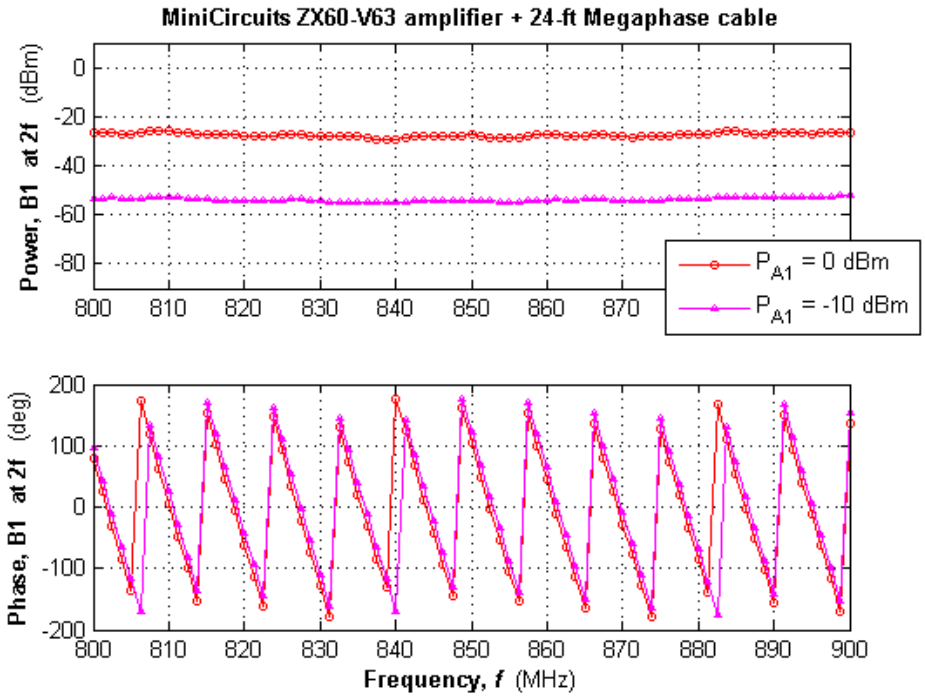

(b)

Fig. 6 Power and phase of 2nd harmonic reflection from the ZX60-V63+ amp input: a) amp connected to Port 1 and b) amp connected through the 24-ft cable to Port 1

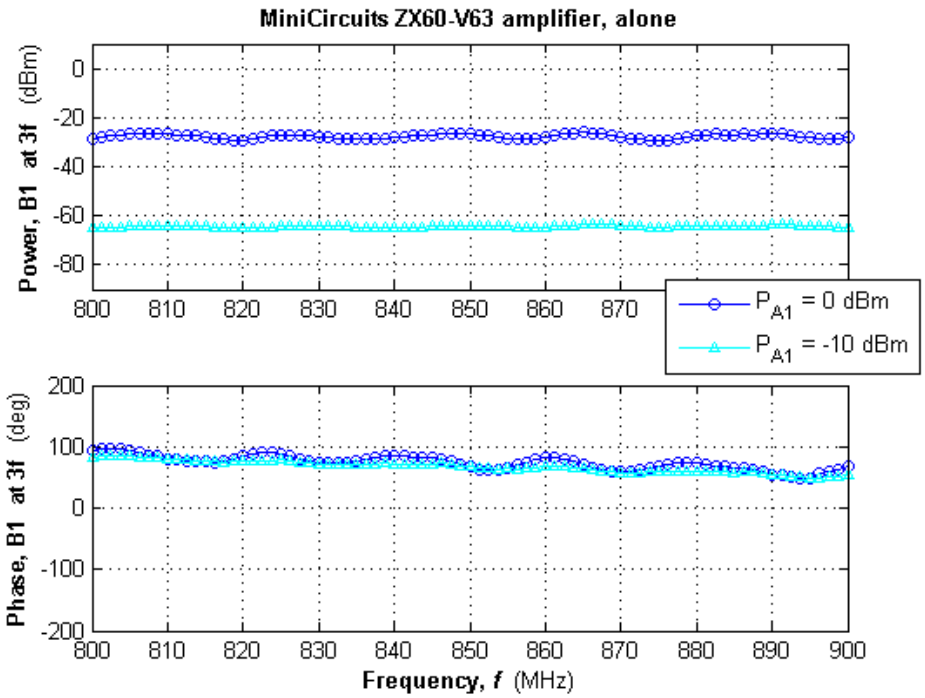

(a)

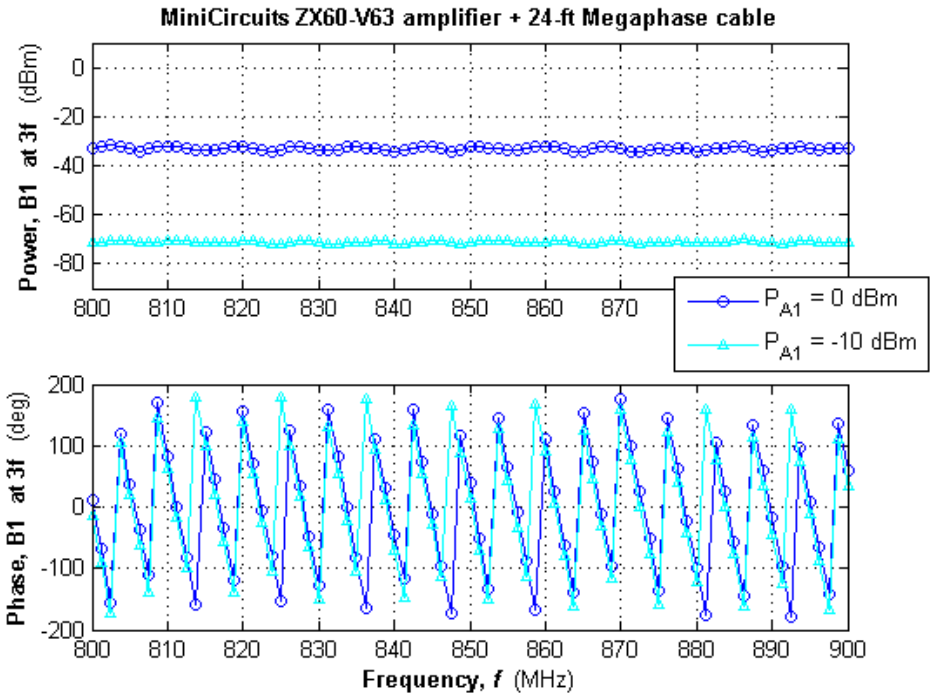

(b)

Fig. 7 Power and phase of 3rd harmonic reflection from the ZX60-V63+ amp input: a) amp connected to Port 1 and b) amp connected through the 24-ft cable to Port 1

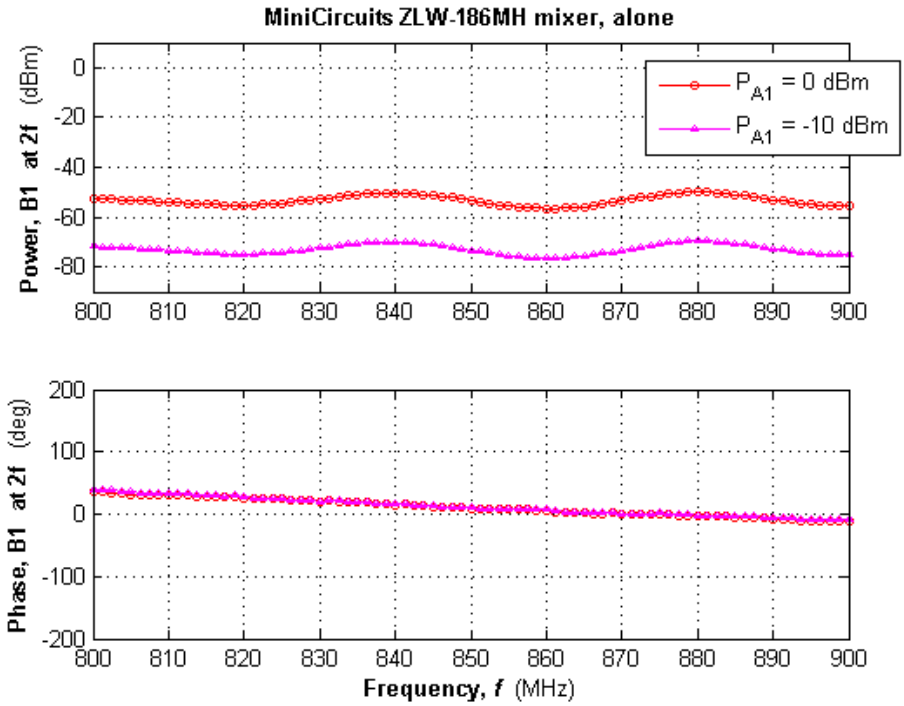

(a)

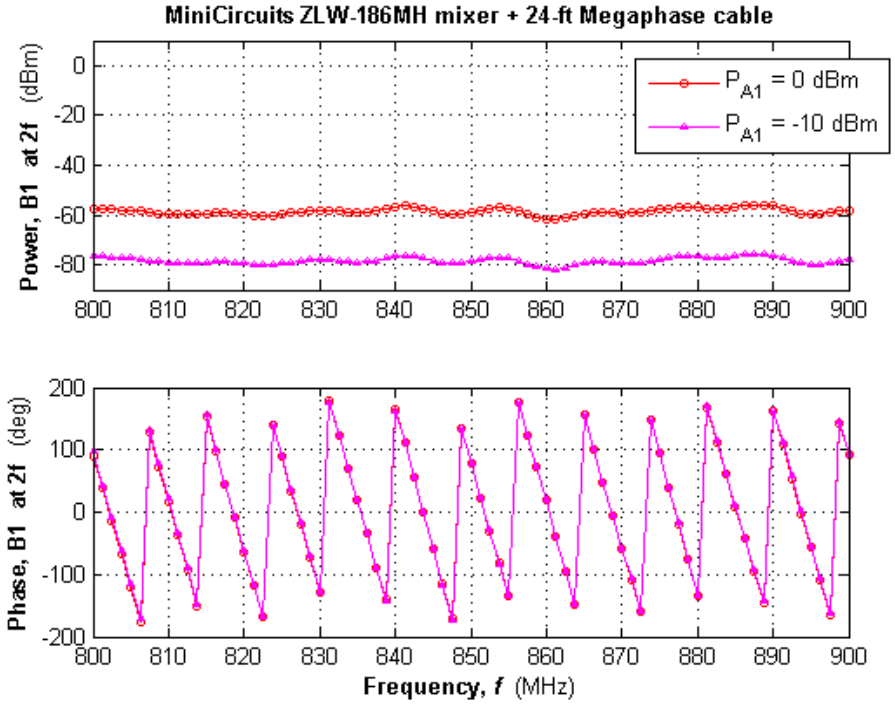

(b)

Fig. 8 Power and phase of 2nd harmonic reflection from the ZLW-186MH mixer RF port: a) mixer connected to Port 1 and b) mixer connected through the 24-ft cable to Port 1

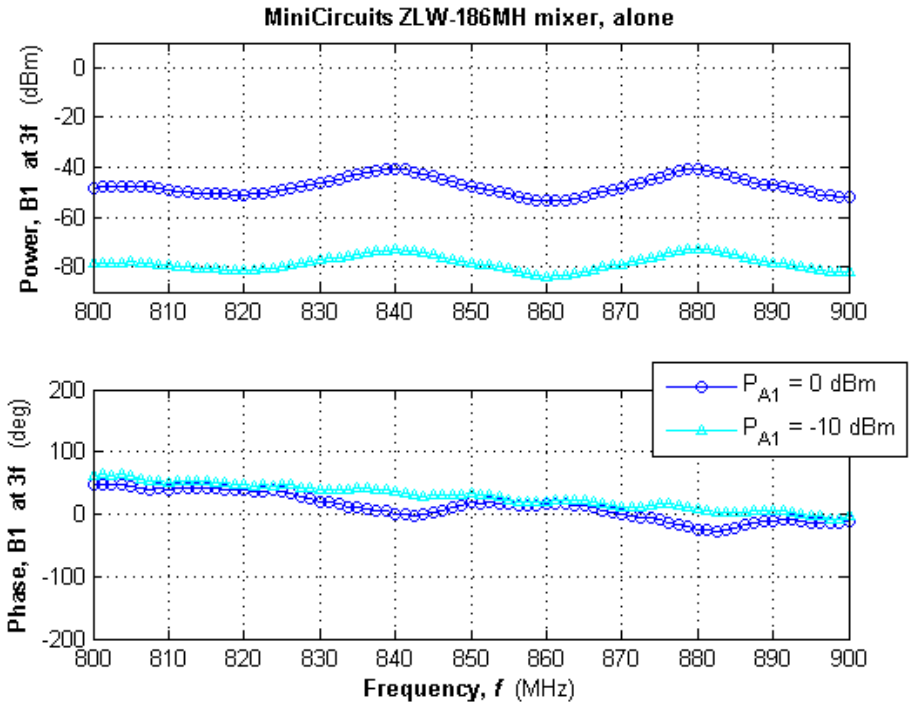

(a)

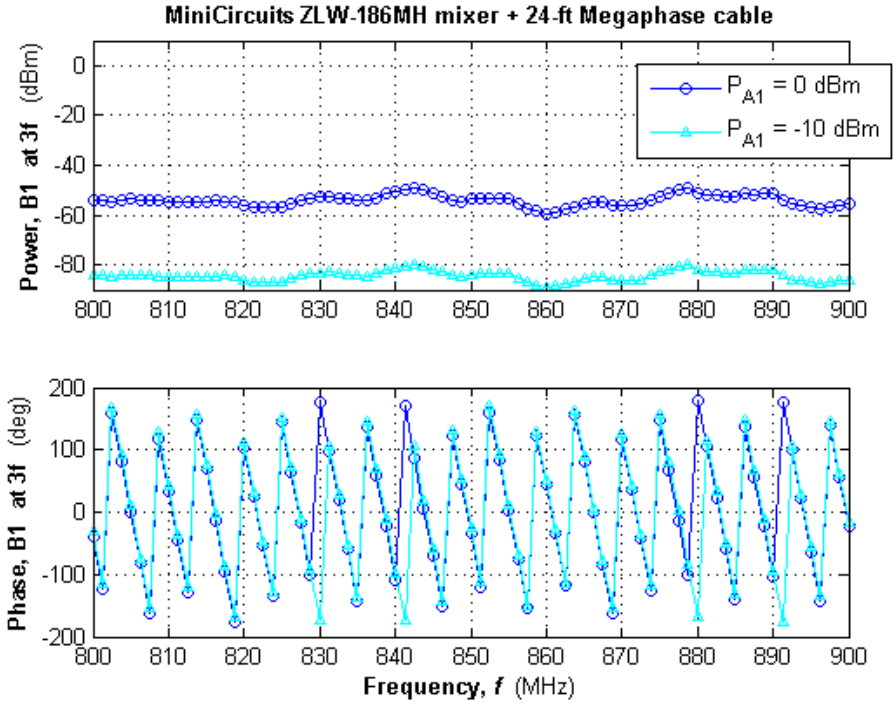

(b)

Fig. 9 Power and phase of 3rd harmonic reflection from the ZLW-186MH mixer RF port: a) mixer connected to Port 1 and b) mixer connected through the 24-ft cable to Port 1

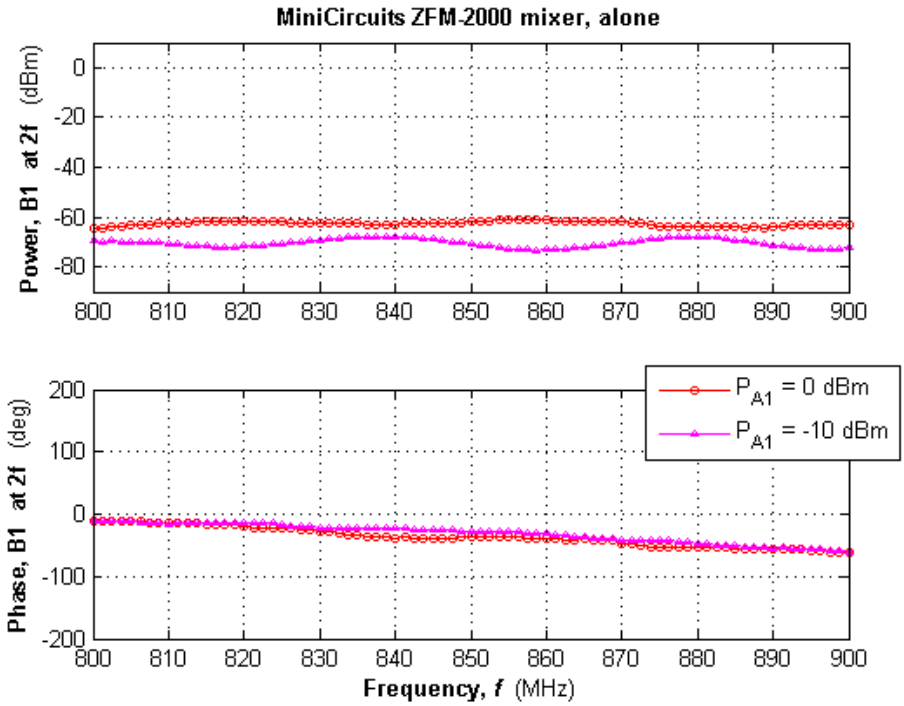

(a)

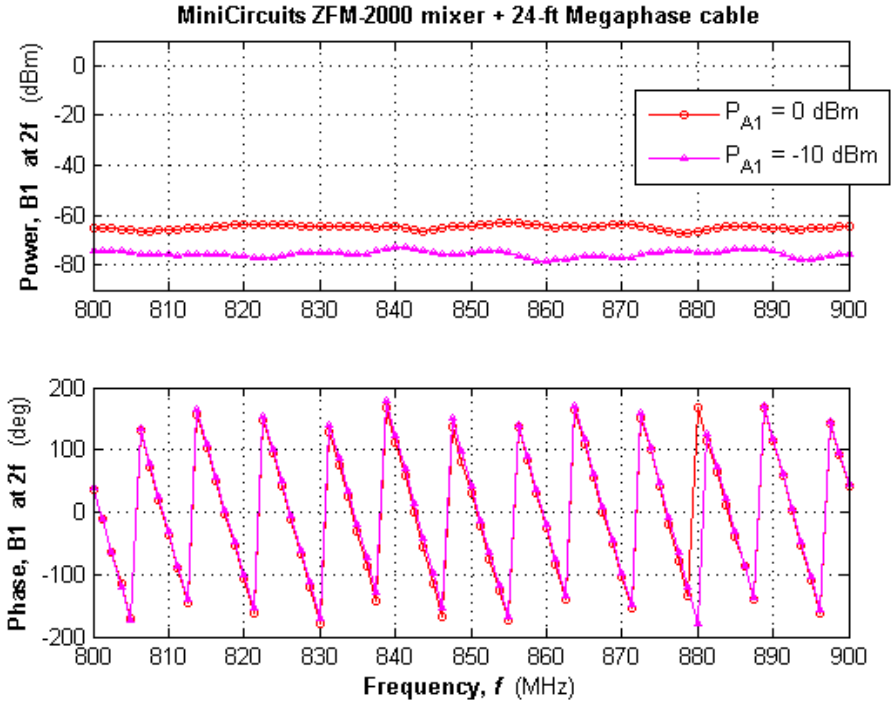

(b)

Fig. 10 Power and phase of 2nd harmonic reflection from the ZFM-2000+ mixer RF port: a) mixer connected to Port 1 and b) mixer connected through the 24-ft cable to Port 1

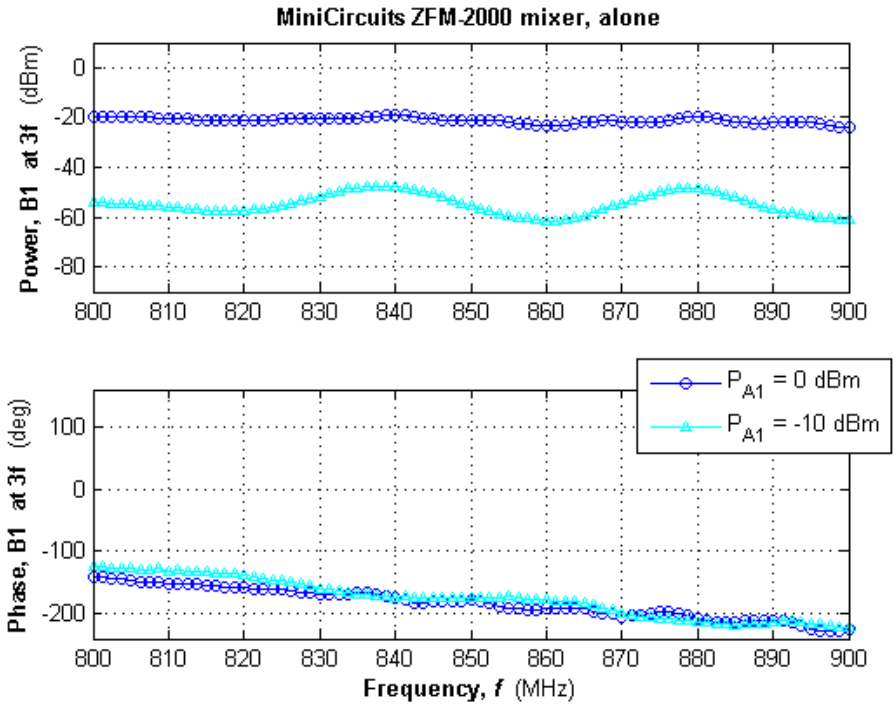

(a)

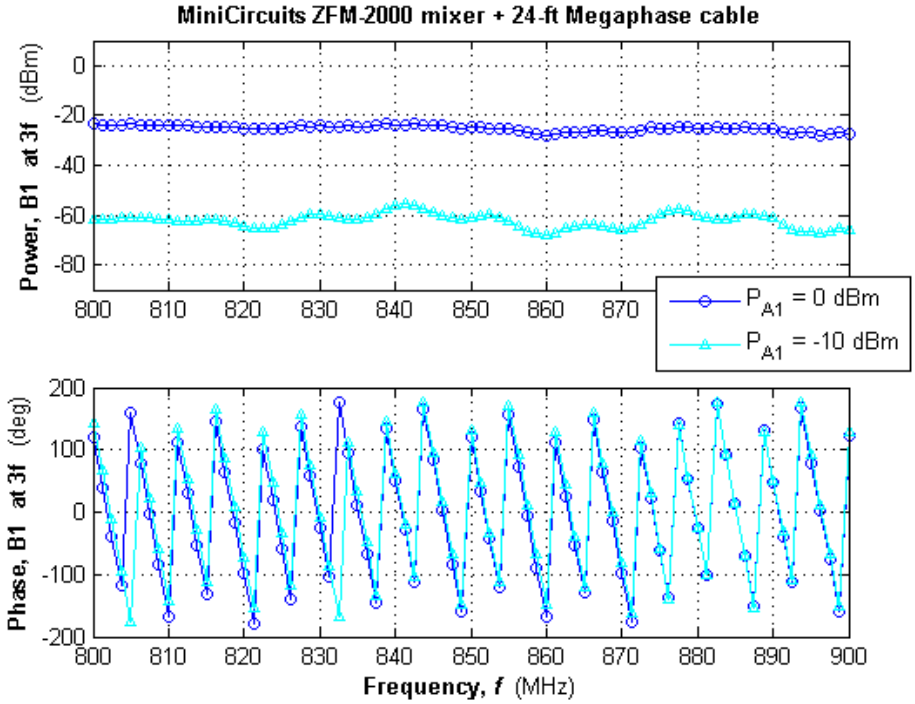

(b)

Fig. 11 Power and phase of 3rd harmonic reflection from the ZFM-2000+ mixer RF port: a) mixer connected to Port 1 and b) mixer connected through the 24-ft cable to Port 1

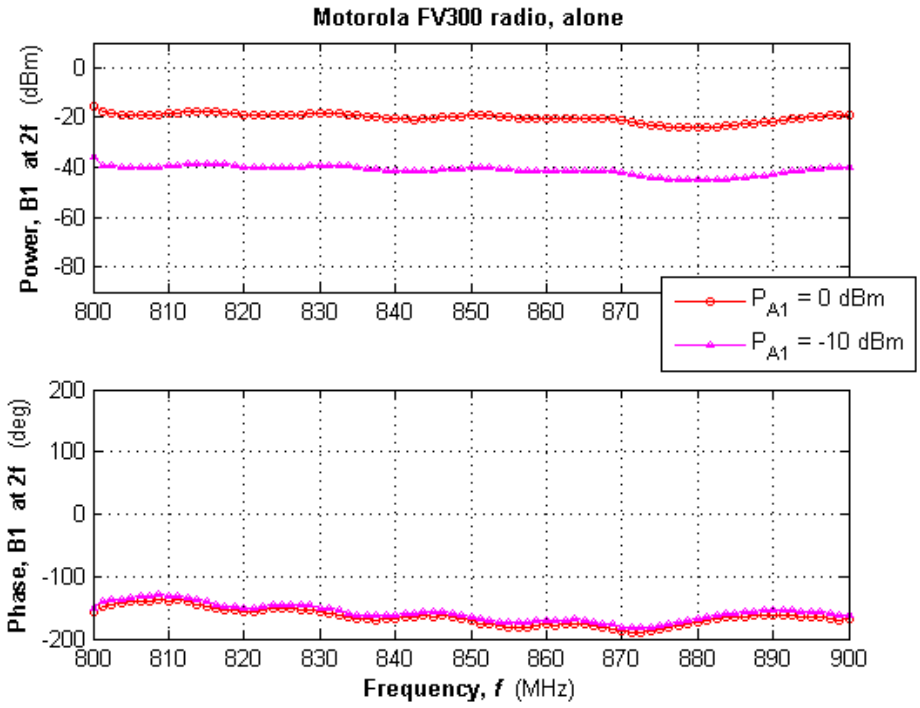

(a)

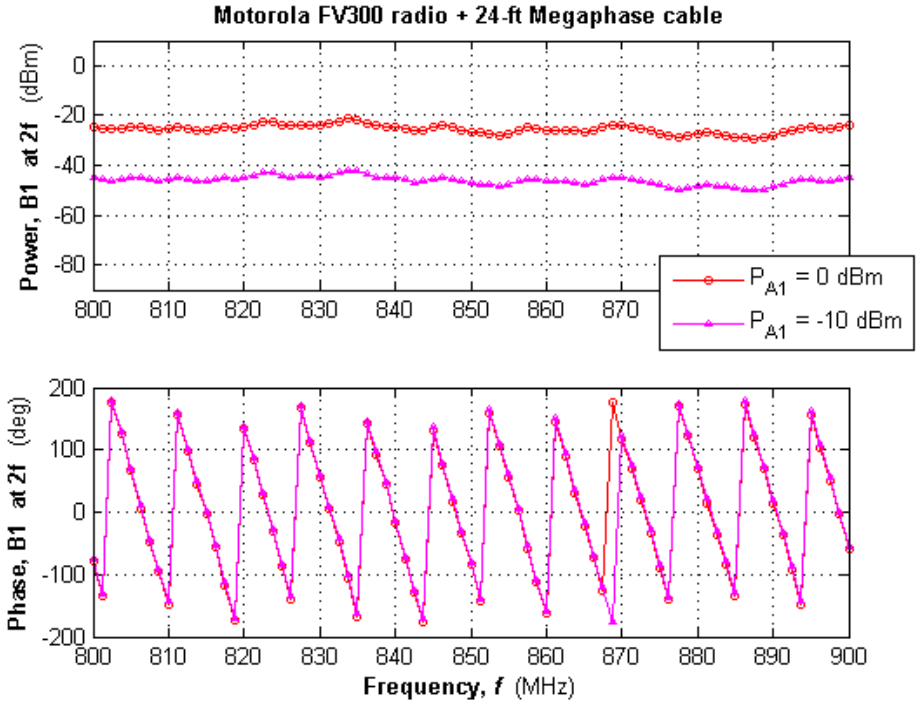

(b)

Fig. 12 Power and phase of 2nd harmonic reflection from the Motorola FV300 radio: a) target connected to Port 1 and b) target connected through the 24-ft cable to Port 1

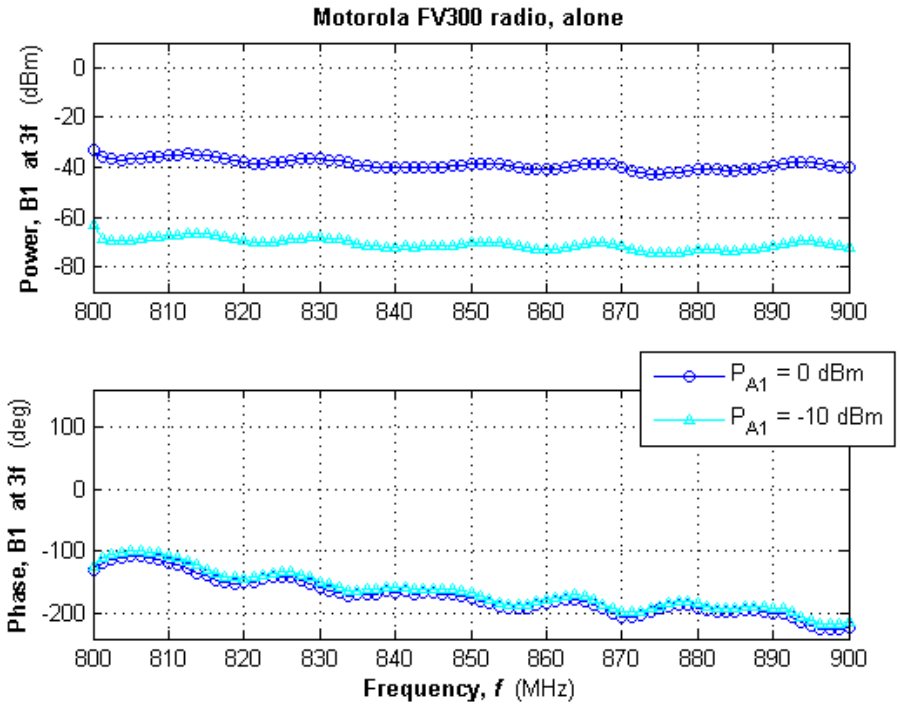

(a)

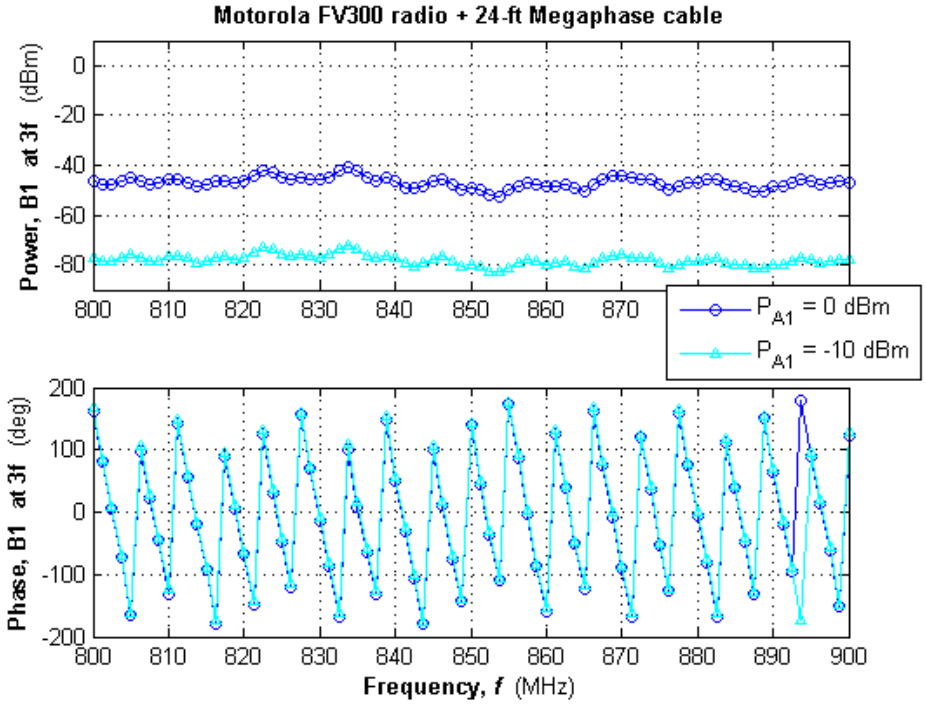

(b)

Fig. 13 Power and phase of 3rd harmonic reflection from the Motorola FV300 radio: a) target connected to Port 1 and b) target connected through the 24-ft cable to Port 1

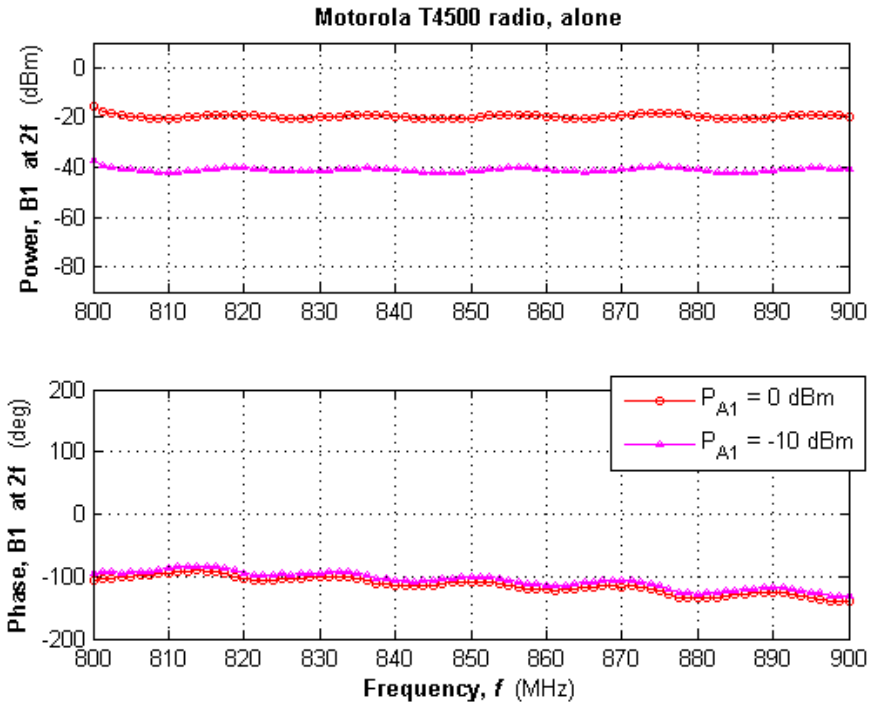

(a)

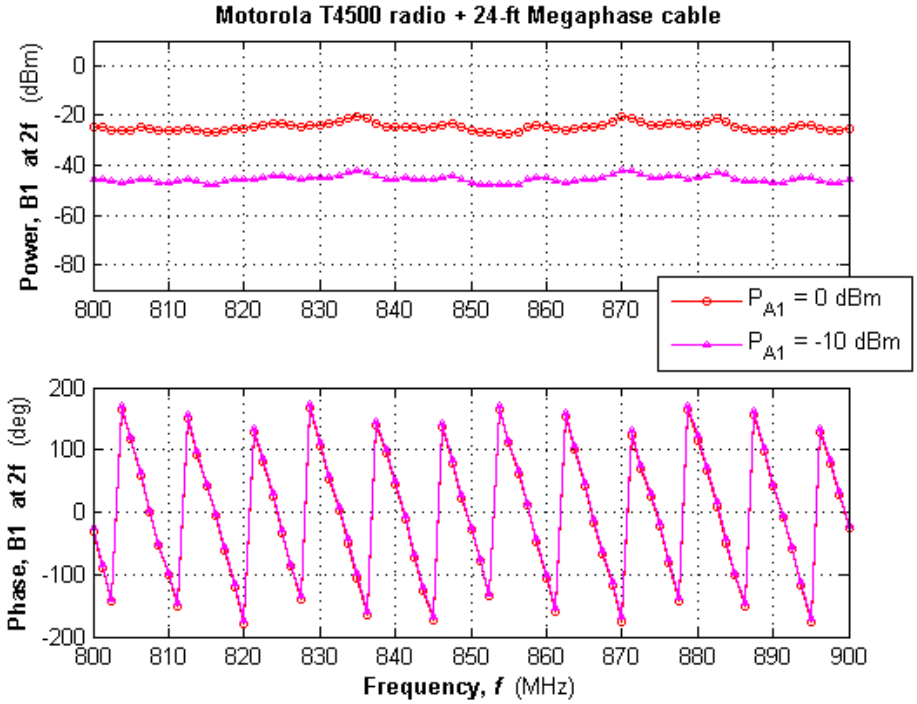

(b)

Fig. 14 Power and phase of 2rd harmonic reflection from the Motorola T4500 radio: a) target connected to Port 1 and b) target connected through the 24-ft cable to Port 1

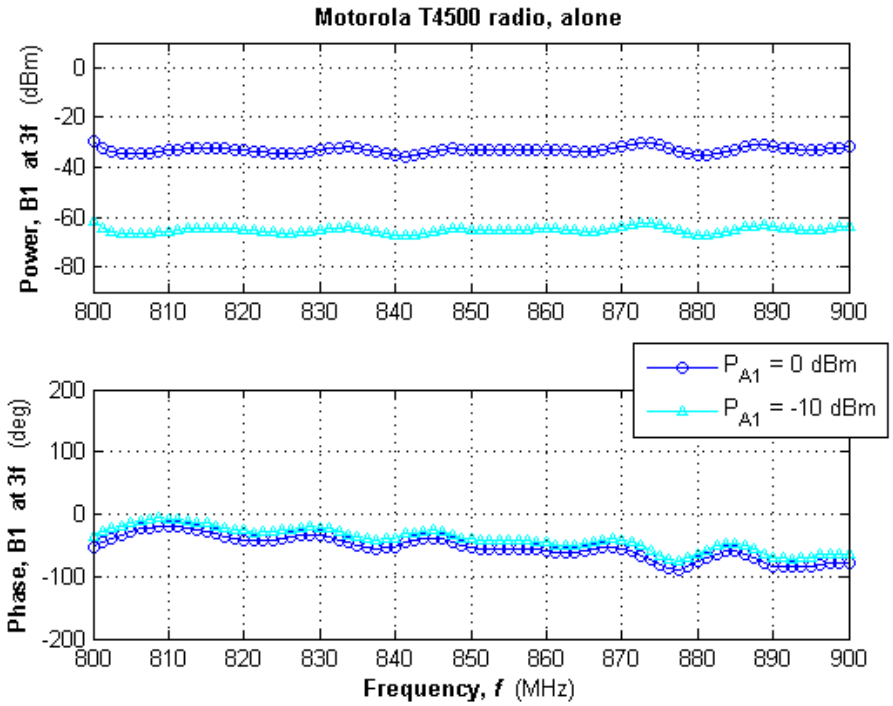

(a)

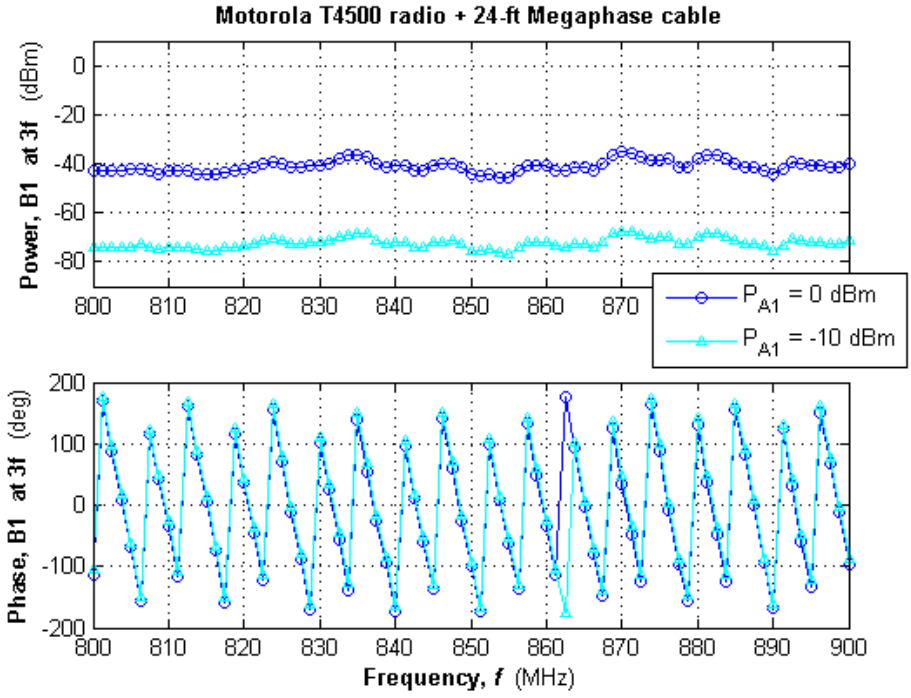

(b)

Fig. 15 Power and phase of 3rd harmonic reflection from the Motorola T4500 radio: a) target connected to Port 1 and b) target connected through the 24-ft cable to Port 1

The assumption that harmonic phase response is constant with frequency is empirically confirmed by the data shown in Figs. 4a through 15a, which delineate a mostly flat phase response when the target is directly connected to Port 1 of the NVNA. Distance can be calculated using this phase response data at either the 2nd or 3rd harmonic of the fundamental. This is shown more clearly in Figs. 16 and 17, which contain the unwrapped phase plots for the FV300 radio (Figs. 12b and 13b) and T4500 radio (Figs. 14b and 15b), respectively, at –10 dBm.

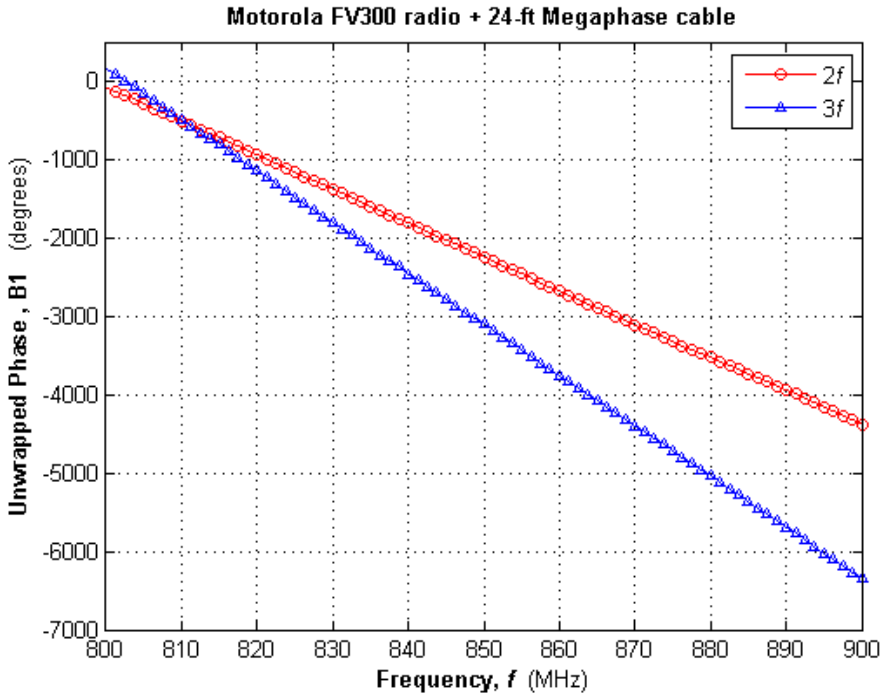

Fig. 16 Unwrapped harmonic phase response for the Motorola FV300

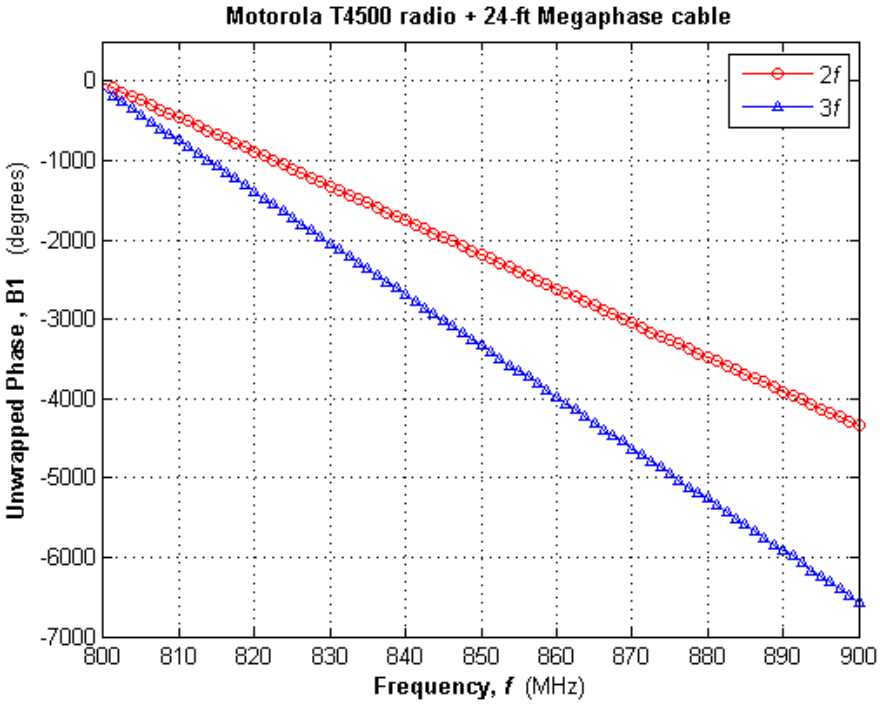

Fig. 17 Unwrapped harmonic phase response for the Motorola T4500

For the FV300 radio, at f = 800 MHz, $\phi_2 = -75°$, and at f = 900 MHz, $\phi_2 = -4375°$. Using a delay of $1/u_p$ = 1.27 ns/ft, as listed in the Megaphase F130 manufacturing specifications,[12] range-to-target may be calculated from the phase response at $2f$ using Eq. 9:

$$d = -\frac{u_p}{2(2)}\left\{\frac{\phi_2(\omega_2)-\phi_2(\omega_1)}{\omega_2-\omega_1}\right\}$$

$$= -\frac{1}{4}\cdot\frac{1\,\text{ft}}{1.27\,\text{ns}}\left\{\frac{\left(-4375°\cdot\frac{\pi}{180°}\right)-\left(-75°\cdot\frac{\pi}{180°}\right)}{(2\pi)\left(900\cdot10^6\,\text{s}^{-1}\right)-(2\pi)\left(800\cdot10^6\,\text{s}^{-1}\right)}\right\} = 23.5\,\text{ft} \quad (10)$$

With MATLAB, this process can be repeated to generate the distance to each tested target from the phase response of the 2nd or 3rd harmonic (Table 1).

Table 1 Range-to-target for devices tested in wireline experiment

Target	*M*	*d*	Target	*M*	*d*
MiniCircuits	2	23.5 ft	MiniCircuits	2	23.6 ft
ZX60-3011+	3	23.4 ft	ZFM-2000+	3	23.7 ft
MiniCircuits	2	23.3 ft	Motorola	2	23.5 ft
ZX60-V63+	3	23.4 ft	FV300	3	23.8 ft
MiniCircuits	2	23.6 ft	Motorola	2	23.6 ft
ZLW-186MH	3	23.6 ft	T4500	3	23.6 ft
			open circuit	1	23.2 ft

Each distance calculated from the phase data is well within 5% of the actual distance (24 ft), confirming that using harmonic phase information to determine range is a valid technique for use in nonlinear radar.

4. Wireless Experiment

Figure 18 shows the next experimental design used to validate the harmonic phase response, a wireless setup slightly more complex than the wired system previously discussed.

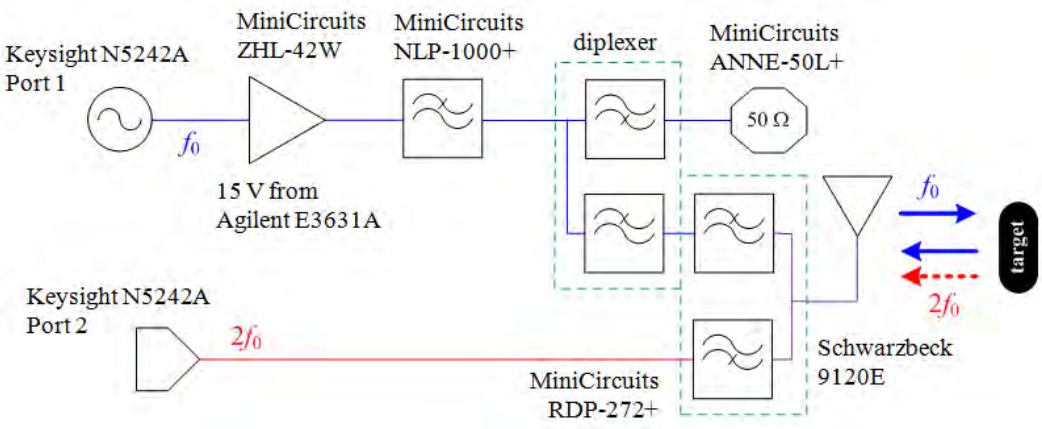

Fig. 18 Wireless experiment setup

Like the wireline tests, this experimental design uses the Keysight NVNA to generate the series of transmit signals, as well as receive the harmonic response; though in this wireless configuration, the received signal enters Port 2, instead of returning to the same port, Port 1, as in the previous design. Similar to the wireline tests, the transmission chain begins with signal generation, amplification, and low pass filtering; however, the wireless configuration employs a much more powerful

amp, the MiniCircuits ZHL-42W, with a gain of roughly 38 dB. Again, the low pass filter acts to attenuate harmonics or artifacts that could be generated during amplification. The first major difference between the wired and wireless setups is the next component in the transmitter chain, a configuration of diplexers that serve 3 functions: 1) divert any remaining harmonics that were not sufficiently attenuated by the first filter to a 50-Ω load, 2) send the desired, artifact-free signal through another series of filters to the vertically aligned Schwartzbeck 9120E antenna to be transmitted to the target, and 3) on the receive chain, attenuating the received fundamental frequency, while passing the harmonic response to Port 2 of the NVNA to be captured.

The targets under test for this wireless experiment were the same handheld Motorola radios used in the wireline experiment, the FV300 and T4500. Both targets were powered-on and tested at distances of both 2 and 3 m, directly in front of the antenna. The bandwidth of frequencies the NVNA generates is 750 to 850 MHz with a step of 0.625 MHz, at a power of –10 dBm.

The same range equations used to determine distance from phase previously derived and described in Eqs. 8 and 9 can be used in the wireless case, with one small modification. Because of the more complex and thus longer transmitter and receive chains, the time it takes to travel the additional distance to and from the NVNA must be accounted for. This, mathematically, simply translates to a subtraction of d_0, or the distance that the signal travels from the NVNAs Port 1 to the antenna plus the distance that the harmonic response traverses from the antenna to the NVNAs Port 2, divided in half.

$$d = -\frac{u_p}{2M}\left\{\frac{\partial}{\partial\omega}\angle\tilde{E}_{\text{rec}}\right\} - d_0 = -\frac{c}{2M}\left\{\frac{\phi_M(f_2)-\phi_M(f_1)}{2\pi(f_2-f_1)}\right\} - d_0 \tag{11}$$

For the radar system used in this experiment, the distance d_0 is 3.2 m. The 2nd harmonic response is shown in Fig. 19 for both radios and 2 different distances.

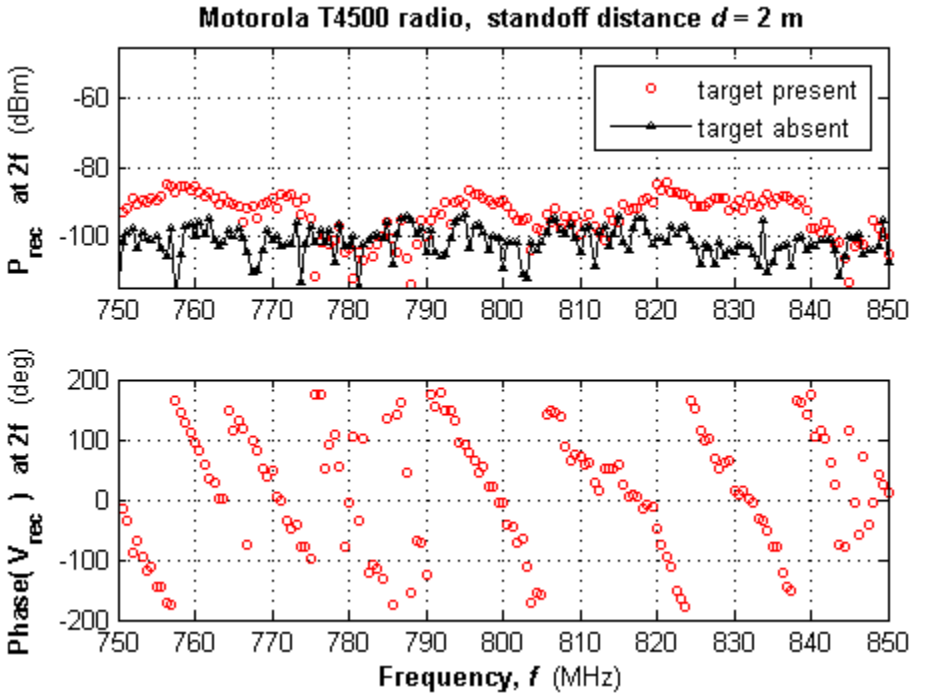

(a)

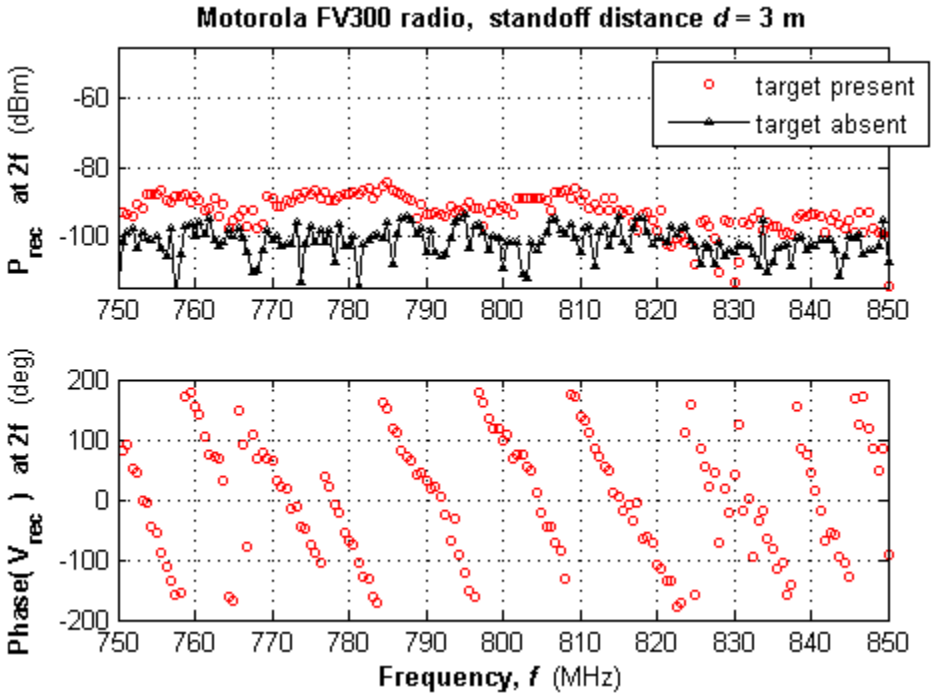

(b)

Fig. 19 Power and phase of 2nd harmonic from the a) Motorola T4500 radio at 2 m away and b) Motorola FV300 radio at 3 m away

Though these data are less strong than their wireline counterpart, range-to-target can still be calculated using Eq. 11, when the target's amplitude response has a sufficient enough signal-to-noise ratio to discern it from the noise floor. Using the 2nd harmonic ($M = 2$) reflected from the T4500 radio and data near 760 MHz (the most visibly straight linear portion of the phase plot):

$$\begin{aligned} d &= -\frac{u_p}{2(2)}\left\{\frac{\phi_M(f_2)-\phi_M(f_1)}{2\pi(f_2-f_1)}\right\} - d_0 \\ &= -\frac{3\cdot 10^8\ \text{m/s}}{4}\left\{\frac{\left(0°\cdot\frac{\pi}{180°}\right)-\left(165°\cdot\frac{\pi}{180°}\right)}{(2\pi)\left(763.8\cdot 10^6\ \text{s}^{-1}-757.5\cdot 10^6\ \text{s}^{-1}\right)}\right\} - 3.2\,\text{m} = 2.2\,\text{m} \end{aligned} \tag{12}$$

The results of the wireless experiment, as shown in Eq. 12, corroborate the data collected in the previous wired experiment. Again, the conjecture that the received harmonics are linear as a function of frequency is verified, so that range can be calculated from the harmonic's phase.

5. Conclusions

Previous nonlinear harmonic radar systems detect targets via transmission of a single frequency ω, stepping (incrementally increasing) this frequency through a wide bandwidth, then listening for a response of the 2nd harmonic 2ω; however, the phase information that this harmonic contains and its relationship to target distance has been largely assumed and unconfirmed. This assumption was verified through 2 experiments, 1 wired and 1 wireless, where the phase of the 2nd and 3rd harmonic of the received electromagnetic wave from nonlinear targets was measured and plotted against the frequency. The result was a linear relationship, in which range-to-target could be calculated from slope.

6. References

1. Kosinski JA, Palmer WD, Steer MB. Unified understanding of RF remote probing. IEEE Sensors. Dec. 2011;11(12):3055–3063.

2. Steer MB, Wilkerson JR, Kriplani NM, Wetherington JM. Why it is so hard to find small radio frequency signals in the presence of large signals. 2012 Workshop on Integrated Nonlinear Microwave and Millimetre-Wave Circuits (INMMIC), pp. 1–3, Sept. 2012.

3. Mazzaro GJ, McGowan SF, Gallagher KA, Sherbondy KD, Martone AF, Narayanan RM. Phase responses of harmonics reflected from radio-frequency electronics. SPIE DSS 2016 Conf. Aug. 2015.

4. Mazzaro GJ, McGowan SF, Gallagher KA, Sherbondy KD, Martone AF, Narayanan RM. Phase Responses of Harmonics Reflected from Radio-Frequency Electronics," in preparation for SPIE DSS 2016, Baltimore, MD, Apr. 2016.

5. Mazzaro GJ, McGowan SF, Gallagher KA, Martone AF, Sherbondy KD. Harmonic phase responses of radio-frequency electronics: wireline test. Adelphi (MD): Army Research Laboratory (US); in preparation.

6. Mazzaro GJ, Ranney KI, Gallagher KA, McGowan SF, Martone AF. Simultaneous-frequency nonlinear radar: hardware simulation. Adelphi (MD): Army Research Laboratory (US); August 2015. Report No.: ARL-TN-0691.

1 (PDF) DEFENSE TECHNICAL INFORMATION CTR DTIC OCA

2 (PDF) DIRECTOR US ARMY RESEARCH LAB IMAL HRA RDRL CIO LL

1 (PDF) GOVT PRINTG OFC A MALHOTRA

11 (PDF) DIRECTOR US ARMY RESEARCH LAB ATTN RDRL SER U T DOGARU M HIGGINS D LIAO A MARTONE D MCNAMARA G MAZZARO K RANNEY M RESSLER K SHERBONDY G SMITH A SULLIVAN